neuroReport

Website publication 13 October 1997

NeuroReport 8, 3513–3518 (1997)

THE response of rat neocortical slices to electrical stimulation at the layer VI/white matter border was recorded using intrinsic signal optical imaging. The optical response of the slice is column-shaped, extends from layer VI to the pial surface, and is strongly correlated with the amplitude of simultaneously recorded evoked potentials. Spectral analysis revealed radially oriented spatial variations in the intensity of the optical signal with a period of 30-60 μm/cycle. Nissl-stained sections of slices also exhibited a radially oriented periodicity in optical density with the same period. We conclude that the periodic variations in the intrinsic optical signal correspond to stimulus-activated minicolumns.

Key words: Intrinsic optical signal; *In vitro*; Minicolumns; Neocortex; Optical imaging

Optical imaging *in vitro* provides evidence for the minicolumnar nature of cortical response

Adam Kohn,[CA] Aluisio Pinheiro,[1] Mark A. Tommerdahl[2] and Barry L. Whitsel[2,3]

Curriculum in Neurobiology and Departments of [1]Statistics, [2]Biomedical Engineering, and [3]Physiology, 155 Medical Research, CB# 7545, University of North Carolina, Chapel Hill, NC 27599-7545, USA

[CA]Corresponding Author

Introduction

Neuronal tissue changes its optical properties when active.[1] The method of intrinsic signal optical imaging makes use of this phenomenon to obtain information about spatially distributed neuronal activity. For instance, maps of orientation selectivity[2] and direction preference[3] have been made from primary visual cortex using intrinsic signal optical imaging *in vivo*. In addition, several groups[4–8] have measured the spatial pattern of activity in hippocampal and neocortical slices using intrinsic signal optical imaging *in vitro*. The available evidence suggests that the intrinsic optical signal (IOS) *in vitro* is primarily a result of a reduction in the extracellular space (ECS) due to astrocytic swelling following extracellular potassium accumulation.[5,7] The reduction in the ECS results in a proportional increase in light transmittance through the tissue. Since extracellular potassium accumulation, and the resultant astrocytic swellings are correlated with the degree and spatial extent of neuronal activity, one can use changes in light transmittance to investigate the spatial characteristics of the distributed response of the neocortical slice to controlled afferent drive.

Optical imaging of neocortical slices has, to date, been used to study only the global components of cortical response. Several groups have reported that the optical response of neocortex to electrical stimulation applied at the layer VI/white matter (WM) border is column-shaped and extends from layer VI to the pial surface.[6–8] In addition, pharmacological manipulations of the receptor systems mediating synaptic activity in the brain slice have been shown to change the global properties of stimulus-evoked optical response. For example, the application of bicuculline was shown to broaden the extent of the column-shaped optical response by reducing pericolumnar inhibition.[6]

In this study we not only confirmed the available observations but, more importantly, made a novel observation concerning the fine spatial structure of the optical response of neocortical slices. In particular, we report that the column-shaped optical response evoked by stimuli applied at the layer VI/WM is not spatially homogeneous. Rather, it displays prominent periodic spatial fluctuations in the 30–60μm/cycle range in a direction parallel to the cortical surface. We propose that these periodic variations in the optical signal correspond to activated minicolumns, the basic modular units of the cortex.[9]

Materials and Methods

Slices (500 μm) were prepared from the sensorimotor cortex of young adult rats (100–125 g). Following preparation, slices were stored in a bath of warmed (30°C), oxygenated (95% O_2/5% CO_2) artificial

cerebrospinal fluid (ACSF) with the following composition (in mM): NaCl, 118; KCl, 4.8; $CaCl_2$, 2.5; $NaHCO_3$, 25; $MgSO_4$, 1.2; KH_2PO_4, 1.2; glucose, 10. After a 2–10 h recovery period, slices were individually transferred to a recording chamber mounted on an inverted microscope. Slices were submerged in the incubation chamber and firmly held in place with a fine mesh. Fresh oxygenated ACSF flowed into the chamber at a rate of 1.5 ml/min. The composition of the ACSF used in the recording chamber was the same as that in the incubation chamber except that it contained 10 μM glycine. Slices were stimulated using a bipolar stimulating electrode (50 μm; FHC) placed at the layer VI/WM border. Stimuli were 0.2 ms square pulses delivered by a constant current stimulator. Evoked potential recordings were made using glass micropipettes filled with 1 M NaCl (impedance 1–2 MΩ) placed ~400 μm from the pial surface (layer III). Evoked potentials were sampled at 20 kHz. A threshold stimulus, defined as the minimum current necessary to generate an evoked potential, was determined for each slice and was usually in the range of 30–50 μA. Using stimuli with intensity values of 1.0–2.5× threshold delivered for 3 s at 10 Hz, we elicited a strong optical response while maintaining slice viability for several hours. For optical imaging, slices were transilluminated using white light from a controlled light source (Oriel) and viewed from below. Images were obtained using a slow-scan CCD camera (Photometrics) mounted on the side port of the microscope. Since we were interested in changes in the light transmittance properties of the slice following stimulation, a reference image was taken 1 s before stimulation began. During each trial an additional 19 images were recorded at intervals of 1.3–1.6 s. The first two images overlapped with the time during which stimuli were delivered; the subsequent images were recorded after stimulation had ended. Difference images were made by subtracting the reference image from each subsequent image. Each image presented in this paper is the sum of those 19 difference images. Although the results presented in this article were present on most of the 19 difference images (frames), we found that averaging the frames improved the signal/noise ratio of the images. Images were selected for spectral analysis if they showed a robust activity pattern and a bell-shaped intensity *vs* position plot (17 of 30 trials recorded were chosen).

Results

Stimulation at the layer VI/WM border led to an optical response in a column-shaped area above the stimulating electrode (Fig. 1A). The optical signal extended from the site of stimulation to near the pial surface with a maximum intensity in the upper layers (see Fig. 2C). The increase in light transmittance was first detected 2–3 s after stimulus onset, peaked 3–5 seconds later, and slowly returned to prestimulus levels over the remaining time during which images were collected (~15 s). Thus, the nature and the time course of the *in vitro* IOS that we recorded was similar to that seen by others using neocortical slices.[6,7] The strength of the optical signal was strongly correlated with both the strength of stimulation and the amplitude of the simultaneously recorded neuroelectric response. As shown in Fig. 1(A,B), a near-doubling of stimulus strength led to an increase in both the amplitude of the evoked potential and the intensity of the optical signal. Neither the shape nor the spatial extent of the IOS was strongly affected by changes in stimulus strength.

Electrical stimuli applied at the layer VI/WM border excite predominantly corticopetal fibers terminating in layer IV. However, stimuli applied at this location also antidromically activate neurons in both the upper and lower layers by activating the corticofugal axons of those neurons. To compare the relative contributions to the IOS of postsynaptic activity from orthodromic activation to that of presynaptic and antidromic activity, we used a modified ACSF lacking calcium and containing twice the normal concentration of magnesium (0 mM Ca^{2+}; 2.4 mM Mg^{2+}). Both the absence of calcium and the high level of magnesium block synaptic transmission while leaving axonal conductance relatively unimpaired. As shown in Fig. 1D, the modified ACSF led to a large reduction in both the intensity of the optical signal and the amplitude of the postsynaptic components of the evoked potential. Reintroducing standard ACSF to the same slice led to a partial recovery of both the optical signal and the evoked potential (Fig. 1E). A similar effect of Ca^{2+}-deficient ACSF has been reported by others.[5,10]

Previous work in our laboratory[11] led us to investigate whether the column-shaped response pattern was spatially homogeneous. Analysis of the fine structure of the optical signal revealed that it clearly

FIG. 1. (A) Left panel: IOS recorded in a neocortical slice elicited by 3 s of 10 Hz stimulation at a current strength of 1.75× threshold. Right panel: Average of the first three evoked potentials recorded during the stimulus train used to elicit the IOS. (B) IOS and evoked potentials from the same slice stimulated at 3.0× threshold. (C–E) IOS and evoked potentials recorded in a different slice (C) while in standard ACSF, (D) 30 min after replacing the standard ACSF with a modified ACSF (0 mM Ca^{2+}, 2.4 mM Mg^{2+}) and (E) after switching back to standard ACSF. The electrode position is indicated by the letter E on (A) and (C); all of the tissues are oriented with the cortical surface to the left of the panel.

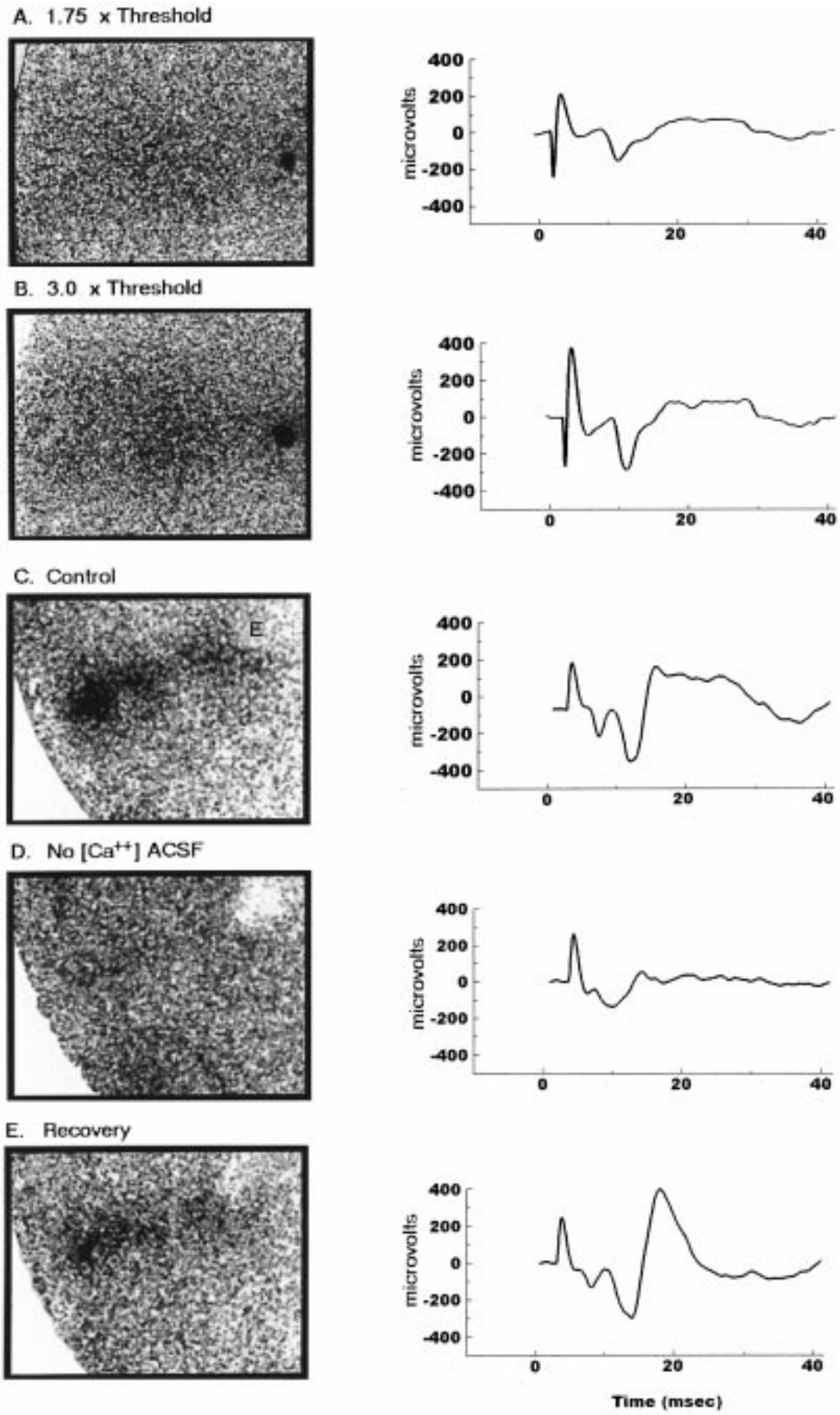
A. 1.75 x Threshold
B. 3.0 x Threshold
C. Control
E
D. No [Ca++] ACSF
E. Recovery
microvolts
400
200
0
-200
-400
0
20
40
Time (msec)

is not. Rather, the columnar IOS consists of periodic fluctuations of intensity in the form of radially-oriented profiles with a center-to-center spacing of 30–60 μm. An example of how the intensity of the IOS varies as a function of the position in the slice is shown in Fig. 2B. IOS intensity at a given position was computed by averaging the intensity values of all pixels in a one-pixel wide bin oriented in a radial direction and extending from the slice surface to layer VI (see Fig. 2A). With the image orientation of Fig. 2A, the intensity at position 0 is calculated using a bin placed at the top of the image and extending from the cortical surface on the left to layer VI on the right of the image; the last position is a similarly oriented bin at the bottom of the image. The resulting intensity *vs* position plot (Fig. 2B, left) shows that there are two strong frequency components to the spatial pattern: a low frequency component reflecting the columnar shape of the IOS; and a superimposed high frequency component. The periodogram at the right of Fig. 2B shows that a significant fraction of the periodic variation in the intensity *vs* position plot is contained in a narrow frequency band of 22–24 cycles/mm (corresponding to a spatial period of 42-45 μm/cycle). Eleven of the 17 images selected for analysis (65%) displayed a prominent spatial frequency component in the stimulus induced IOS in a narrow range between 17 and 33 cycles/mm (30–60 μm/cycle). We propose that these periodic fluctuations in the IOS reflect activated minicolumns.

To be sure that the periodic spatial variations in the optical signal are not an artifact of stimulation or of the imaging system, several controls were carried out. First, we checked for periodic variations in the IOS using bins oriented parallel to the cortical surface (i.e. perpendicular to the orientation of the bins used above; right panel in Fig. 2A). Since minicolumns are radial structures, our expectation was that if the periodicity in the IOS was attributable to minicolumns, there should not be strong periodic variations in the IOS in this direction. Figure 2C shows an intensity distribution (left panel) and a periodogram (right panel) constructed from the same image as in Fig. 2A but this time using bins parallel to the slice surface. In this case, the intensity *vs* position plot shows that the intensity of the IOS decreases as one moves away from the slice surface and that there are some high spatial frequency components to the IOS. The accompanying periodogram, however, clearly shows that these high spatial frequency components do not include a particularly strong spatial frequency component in the minicolumn range (30–60 μm/cycle). As a second control, we checked for the presence of periodic variations in the optical density of Nissl-stained sections of the slices from which the functional images were obtained. If the periodic variations of the IOS are a functional manifestation of the well known radial arrangement of cortical neurons, one would expect to see periodic fluctuations in the optical density of Nissl-stained sections on a similar spatial scale. Figure 2D (left) shows a Nissl-stained section obtained from the slice shown in Fig. 2A. The accompanying periodogram, obtained using radially oriented bins, shows the presence of a strong spatial frequency component in the minicolumn range centered at precisely the same spatial frequency present in the optical images. As a final control, a different slice was imaged at several different magnifications. Changes in the magnification altered the number of pixels per cycle (not shown), but did not shift the periodogram peak in the minicolumn range: at all three magnifications (4×, 6.3× and 10×), there was a prominent peak between 29 and 33 cycles/mm (spatial period of 30–34 μm/cycle).

Discussion

Periodic variations of high spatial frequency in the IOS are evoked in a neocortical slice by stimulation at the layer VI/WM border. The frequency of these spatial variations in IOS intensity indicates the presence of a repeating radially oriented structure with a center-to-center spacing equal to that of the cortical minicolumn. That these spatial variations in the IOS do indeed correspond to activated minicolumns is supported by the following observations: (1) the spatial scale of the periodicity does not change with changes in the magnification used to obtain the optical images; (2) there is no minicolumn-scale periodicity in the IOS in the radial direction; and (3) Nissl-stained sections of slices reveal periodic fluctuations of optical density having the same orientation and precisely the same spatial frequency as those seen in the IOS. It is important to note that the variations in the IOS can not be a simple

FIG 2. (A) Left panel: IOS in a neocortical slice elicited by 3 s of 10 Hz stimulation at a current strength of 2.5× threshold. The electrode position is indicated by an E; the tissue is oriented with the cortical surface to the left of the panel. Right panel: The orientation of the bins used to produce (B) and (C). (B,C) Left panel: Intensity *vs* position plots obtained by averaging all pixel values in a one-pixel wide bin; the orientation of the bins for the two plots is shown in (A); Right panel: Periodograms of the intensity *vs* position plots. (D) Left panel: Image of a Nissl-stained section; Right panel: Periodogram of the optical density distribution of the stained section. (E) Periodograms obtained from three successive trials in the same slice at three different magnification factors. The lowest frequency peaks (1–3 cycles/mm) in all periodograms have been removed for clarity. All periodograms have been normalized so that the sum of the spectral energy in all bins is equal to 100%.

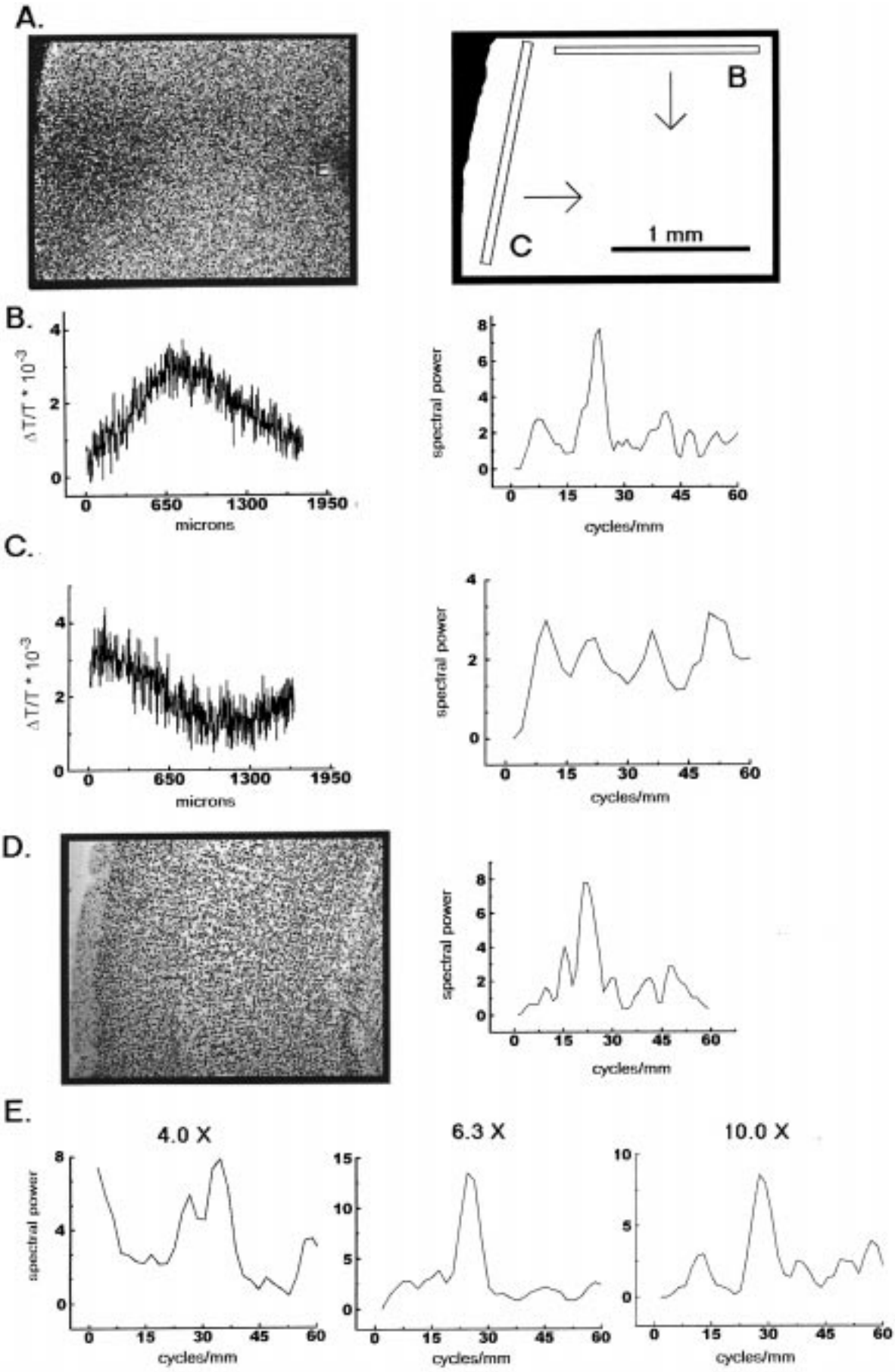
A.
B
C
1 mm
B.
ΔT/T * 10^-3
microns
spectral power
cycles/mm
C.
ΔT/T * 10^-3
microns
spectral power
cycles/mm
D.
spectral power
cycles/mm
E.
4.0 X
6.3 X
10.0 X
spectral power
cycles/mm

anatomical artifact since the optical images are made by subtracting a reference image of each slice. Rather, the presence of minicolumn-scale periodicities in the IOS is a functional manifestation of the anatomical structure of the cortex.

That the spatial pattern of activity evoked in cortex by afferent drive is heterogeneous has been observed previously. McClasland and Woolsley[12] reported that 2-deoxyglucose (2DG) labeling in barrel cortex shows radially oriented inhomogeneities within a single barrel corresponding to groupings of minicolumns. 2DG studies[11] of labeling in the somatosensory cortex of cats and monkeys have shown that the heterogeneous pattern of metabolic labeling is periodic with a spatial period of 35–50 μm/cycle. In those experiments, Nissl stained sections of monkey and cat somatosensory cortex confirmed that the periodic variations in the 2DG pattern correspond to activated minicolumns. The present report complements these findings by showing that a similar phenomenon is present in optical images.

The minicolumnar structure of the cortex seen in Nissl-stained sections is a direct result of the ontogenic developmental mechanism proposed by Rakic.[13] Since neurons migrate along radial glial cells from the neural tube to their final location in the cortex, their final arrangement is a vertical stack of cells which extends from the cortical surface to the subcortical white matter and contains about 110 cells. These vertical stacks also correspond to the pyramidal cell modules defined by Peters.[14] In functional terms, the cells in a minicolumn display very similar response and receptive field (RF) characteristics since thalamocortical afferent input to layer IV is distributed throughout the column by spiny stellate cells in that layer. Neurophysiological evidence for this view comes from fine scale single electrode recordings *in vivo*.[15–18] In those experiments, recordings using radial penetrations show little change in RF properties while tangential penetrations result in a rapid shift in the RF location of neighboring neurons as one records from neighboring minicolumns. If these rapid changes in RF properties correspond to recordings from distinct minicolumns, then neighboring minicolumns must have distinct afferent and cortical inputs. Thus, one would expect that different spatial and temporal parameters of afferent drive *in vitro* will result in different patterns of minicolumn activation. This hypothesis is currently under investigation in our laboratory.

Conclusion

Spectral analysis of *in vitro* optical images reveals a strong periodicity in the intensity of the intrinsic signal on a spatial scale of 30–60 μm/cycle. This periodicity corresponds to alternating high and low radially oriented bands of the intrinsic signal; a similar periodicity was not found in a perpendicular direction. This periodicity is also present in Nissl-stained sections where it clearly corresponds to anatomical minicolumns. Changes in the magnification used to obtain the images does not change the spatial scale of the periodicity. We propose that this periodicity corresponds to activated minicolumns. Whether changes in the spatial and temporal properties of afferent drive result in different patterns of minicolumn activity is now under investigation.

References

1. Grinvald A, Frostig RD, Lieke E and Hildesheim R. *Physiol Rev* 68, 1285–1366 (1988).
2. Bonhoeffer T and Grinvald A. *Nature* 353, 429–431 (1991).
3. Weliky M, Bosking WH and Fitzpatrick D. *Nature* 379, 725–728 (1996).
4. Andrew RD and MacVicar BA. *Neuroscience* 62, 371–383 (1994).
5. MacVicar BA and Hochman D. *J Neurosci* 11, 1456–1469 (1991).
6. Dodt HU, Darcangelo G, Pestel E, and Zieglgansberger W. *NeuroReport* 7, 1553–1558 (1996).
7. Holthoff K and Witte OW. *J Neurosci* 16, 2740–2749 (1996).
8. Holthoff K, Dodt HU, and Witte OW. *Neurosci Lett* 180, 227–230 (1994).
9. Mountcastle VB. An organizing principal for cerebral function: The unit module and the distributed system. In: Edelman GM and Mountcastle VB, eds. *The Mindful Brain*. Cambridge: MIT Press, 1978: 7–51.
10. Albowitz B and Kuhnt U. *Exp Brain Res* 93, 213–225 (1993).
11. Tommerdahl M, Whitsel BL, Nakhle B and Favorov O. *Cerebr Cortex* 3, 399–411 (1993).
12. McCasland JS and Woolsley TA. *J Comp Neurol* 278, 555–569 (1988).
13. Rakic P. *Science* 241, 170–176 (1988).
14. Peters A and Yilmaz E. *Cerebr Cortex* 3, 49–68 (1993).
15. Favorov OV and Whitsel BL. *Brain Res Rev* 13, 25–42 (1988).
16. Favorov OV and Diamond ME. *J Comp Neurol* 298, 97–112 (1990).
17. Abeles M and Goldstein MH. *J Neurophysiol* 33, 172–187 (1970).
18. Albus K. *Exp Brain Res* 24, 181–202 (1975).

ACKNOWLEDGEMENTS: This work was supported by the Whitehall Foundation. Special thanks to Carol Metz, Calvin Wong, and Rebekah Mosher for technical assistance.

Received 24 July 1997; accepted 2 September 1997